# Properties of the CsPbBr₃ Quantum Dots Treated by O₃ Plasma for Integration in the Perovskite Solar Cell

Sh. Sousani, Z. Shadrokh, M. Hofbauerová, J. Kollár, M. Jergel, V. Nádaždy, M. Omastová, E. Majková

***Abstract***—In this paper, we discuss the preparation and impact of post-treatment procedures, including purification, passivation, and ligand exchange, on the formation and stability of halide perovskite quantum dots (PQDs). CsPbBr₃ quantum dots were synthesized via the conventional hot-injection method using cesium oleate, PbBr₂, and oleylamine (OAm) & oleic acid (OA) and didodecyldimethylammonium bromide (DDAB) as ligands. Characterization by scanning transmission electron microscopy (STEM) confirms the QDs' cubic shape and monodispersity with an average size of 10-14 nm. The photoluminescent (PL) properties of perovskite quantum dots/CH₃NH₃PbI₃ perovskite (PQDs/MAPI) bilayers with OAm&OA and DDAB ligands spin coated on Indium Tin Oxide (ITO) substrate were explored. The impact of ligand type and oxygen plasma treatment on linear optical behaviour and PQDs/MAPI interface formation in ITO/PQDs/MAPI perovskite structures was examined. The obtained results have direct implications for selection of suitable ligands and processes for photovoltaic applications and enhancing their stability.

***Keywords***—Perovskite quantum dots, ligand exchange, photoluminescence, O₃ plasma.

## I. INTRODUCTION

PQDs represent a ground-breaking class of nanoscale semiconductors, combining the unique crystal structures of perovskites with the quantum confinement effects characteristic of quantum dots. These versatile materials offer unprecedented opportunities in optoelectronics and nanotechnology thanks to their tunable bandgaps, high photoluminescence efficiencies, and excellent colour purity. The discovery of PQDs in 2015 marked a turning point in the search for alternative quantum dots, as they overcame several limitations associated with traditional materials. For example, unlike metal chalcogenide quantum dots, PQDs do not require surface passivation, making them more robust against imperfections and easier to integrate into optoelectronic devices. Additionally, PQDs can be synthesized using scalable and cost-effective methods, opening doors to widespread industrial adoption. This burgeoning area of research holds great promise for transformational advancements in numerous sectors, including displays, light-emitting diodes, solar cells, and sensors.

Understanding the fundamental principles controlling PQDs behaviour at the atomic scale is crucial for harnessing their full potential and driving innovation in modern technology. PQDs have the potential to increase the performance of the perovskite solar cells (PSCs) [1]. The integration of PQDs into PSCs can extend the absorption range, enhance photon harvesting and device efficiency. In addition, PQDs can stabilize the device structure by passivating surface defects and traps in the perovskite layer and enhance its stability. The integration of PQDs into PSCs is strongly affected by the type of ligands on the surface of PQDs. The ligands affect the charge transport properties of PQDs, as well as the formation of well-defined interfaces and stability of PSCs. In PQD synthesis, the choice of ligands plays a crucial role in determining the structural, optical, and electronic properties of the resulting PQDs. Two commonly used ligands, OAm&OA and DDAB, have been extensively studied for their influence on PQD morphology, stability, and device performance. OA and OAm are known for their ability to passivate surface defects and improve the stability of PQDs, while DDAB offers enhanced charge transport properties and facilitates the formation of well-defined interfaces in PSCs [2]. Ding et al. conducted a study focusing on optimizing ligands to improve the efficiency of CsPbBr₃ PQDs. Their research showcased significant enhancements in luminescent properties and device performance achieved through systematic ligand engineering. These results highlight the critical role of ligand selection and manipulation in customizing the optical and electronic characteristics of PQDs [3]. This study explores the synthesis of CsPbBr₃ quantum dots (QDs) using cesium oleate and PbBr₂ with two different ligands: OAm&OA and DDAB, by the hot-injection method. STEM confirms the cubic shape and monodispersity of the PQDs, with an average size of 10-14 nm. PL properties of PQDs/perovskite bilayers with OAm&OA and DDAB ligands were investigated. The impact of ligand type and oxygen plasma treatment on PQDs/MAPI interface formation was studied, revealing significant effects on surface states and PL behaviour.

## II. EXPERIMENTAL SECTION

### A. Synthesis of Perovskite Quantum Dots

The PQDs for our study were synthesized following the hot-injection method described by Bi et al. [4]. To synthesize CsPbBr₃ QDs, 10 mL of 1–octadecene and 0.138 g of PbBr₂ were loaded into a 100 mL three-necked flask and dried under vacuum conditions for 1 h at 120 °C. Then, the flask was cleansed with N₂, and the solution in the flask was loaded in N₂. Thereafter, 1 mL of OA and 1 mL of OAm were added to the above solution under N₂. The flask was degassed under vacuum

Sh. Sousani, Z. Shadrokh, M. Hofbauerová, M. Jergel, V. Nádaždy and E. Majková are with Institute of Physics, Slovak Academy of Sciences, Dúbravská cesta 9, 84511 Bratislava, Slovak Republic (e-mail: shima.sousani@savba.sk).

J. Kollár and M. Omastová are with Polymer Institute, Slovak Academy of Sciences, Dúbravská cesta 9, 84541 Bratislava, Slovak Republic.

World Academy of Science, Engineering and Technology
International Journal of Energy and Power Engineering
Vol:18, No:7, 2024

to dissolve $PbBr_2$ completely and remove $H_2O$ and $O_2$. The flask was held under a constant $N_2$ flow, and the mixture was heated at 180 for $CsPbBr_3$. Subsequently, the Cs-oleate (0.0625 M, 1.6 mL) precursor was swiftly injected into the reaction mixture. After 5 s, the reaction was ended by cooling the solution to room temperature. The $CsPbBr_3$ QDs were purified by adding MeOAc and then the mixture was centrifuged at 8000 rpm for 5 min. Followed by discarding the supernatant, 3 mL of hexane was added to redisperse the precipitation which contains QDs. The $CsPbBr_3$ QDs were then precipitated by adding MeOAc and centrifuged at 8000 rpm for 2 min. Finally, The QD colloidal solution was dispersed in 3 mL of hexane and centrifuged at 4000 rpm for 5 min to remove any insoluble aggregates.

### B. Sample's Preparation

The PQDs solution was spin coated onto ITO substrates at a speed of 2000 rpm for 20 seconds, followed by annealing at 150 °C for 1 minute. Subsequently, the samples were exposed to $O_3$ plasma for 5, 10, and 15 seconds. The perovskite layer was prepared by synthesizing a precursor solution comprising a mixture of 507 mg of lead iodide (PbI2) and 175 mg of methyl ammonium iodide (MAI) dissolved in 900 µl of dimethyl formamide and 100 µl of dimethyl sulfoxide. This solution was stirred overnight at room temperature. The control perovskite precursor solution was deposited onto PQDs-covered substrates using a two-step spin coating process. Initially, the solution was spun at 1000 rpm for 5 seconds followed by 5000 rpm for additional 45 seconds in a glovebox environment. Simultaneously with the start of the first 5 second step, 200 µl of chlorobenzene was applied to facilitate perovskite crystallization. Subsequently, the ITO/PQDs/perovskite substrates were annealed at 50 °C for 2 minutes in darkness and subsequently at 100 °C for 20 minutes within the glovebox.

### C. Characterization and Measurements

STEM imaging was done to visualize the microstructure and composition of the samples. UV-Vis-NIR spectrophotometer (SolidSpec–3700 Shimadzu, Japan) was employed to analyse the optical absorption properties of the materials. The PL spectroscopy was utilized to investigate the emission characteristics of the materials. These measurements provided insights into the electronic and optical properties of the samples.

## III. RESULTS AND DISCUSSION

According to STEM images (Fig. 1), the prepared $CsPbBr_3$ QDs present relatively monodisperse cubic structure with an average size of about 10-14 nm.
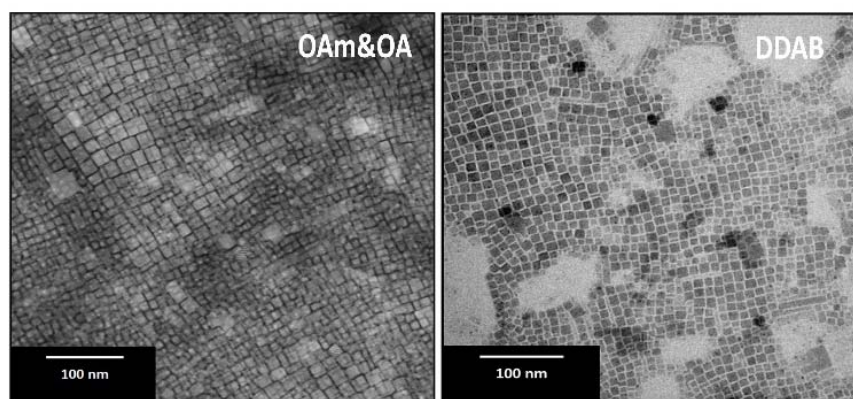


Fig. 1 STEM images of cubic-shaped $CSPbBr_3$ QDs

The UV-Vis absorption spectra of $CsPbBr_3$ QDs with different ligands provide insight into their optical and structural properties. The distinct absorption edges observed for OAm&OA $CsPbBr_3$ QDs at 513 nm and DDAB $CsPbBr_3$ QDs at 490 nm correspond to band gaps of 2.38 eV and 2.33 eV, respectively (Fig. 2). These differences in absorption edge positions are indicative of variations in the band structures and electronic transitions in the QD systems, influenced by the ligand environment and quantum confinement effects [5].
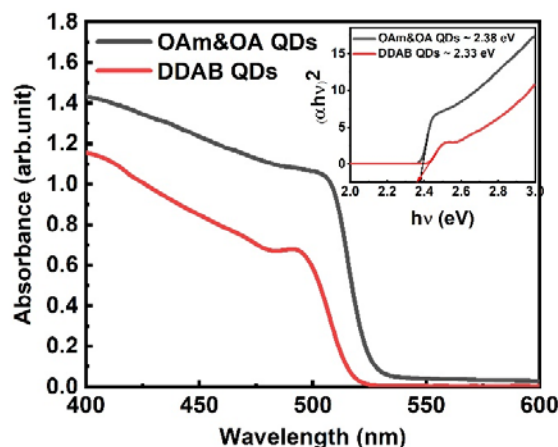


Fig. 2 UV-vis absorption spectra (inset: Tauc plot for calculation of band gap energy with OAm&OA and DDAB ligands separately

World Academy of Science, Engineering and Technology
International Journal of Energy and Power Engineering
Vol:18, No:7, 2024

The PL spectra of OAm&OA $CsPbBr_3$ QDs exhibit a slight redshift compared to DDAB $CsPbBr_3$ QDs, reflecting differences in the QD size distributions and quantum confinement effects (Fig. 3). The broader full width at half maximum (FWHM) of the PL spectrum for DDAB $CsPbBr_3$ QDs suggests a wider range of QD sizes and less uniformity compared to OAm&OA $CsPbBr_3$ QDs. In particular, this broadening is attributed to variations in QD sizes and subsequently to various bandgap energies within the DDAB-capped QD ensemble [6].
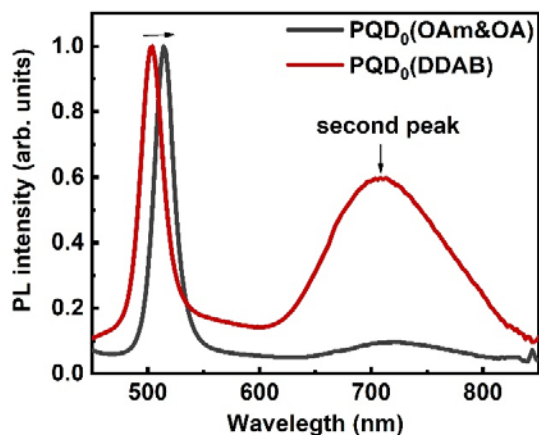


Fig. 3 PL spectra of CsPbBr3 QDs with OAm&OA and DDAB ligands

The occurrence of a secondary peak in the PL spectra of both types of perovskite QDs thin films indicates the presence of surface states. These surface states are strongly affected by the $O_3$ plasma treatment.

In Fig. 4, a distinct impact of plasma treatment duration on CsPbBr3 QD thin films can be observed. In particular, plasma treatment of the OAm&OA CsPbBr3 QDs results in a uniform size distribution, indicating ligand removal and enhanced homogeneity, as evidenced by the disappearance of the second PL peak. On the contrary, DDAB CsPbBr3 QDs display intensity fluctuations in the second peak, suggesting an interplay among ligand removal, PQDs aggregation and changes in surface properties.

Similarly, the impact of $O_3$ plasma treatment on PQDs is different for two ligands. The PQDs with DDAB ligand experience a blue shift in the PQDs peak and a non-monotonous change in the amplitude of the surface states peak due to $O_3$ exposure. On the contrary, PQDs with OAm&OA ligand show no shift in the PQDs peak under the same treatment.

Furthermore, prolonged treatment times lead to surface degradation of the PQDs film and the deterioration of organic ligands, consequently resulting in increased aggregation. This result highlights the critical role of ligands in governing PQDs stability and morphology.
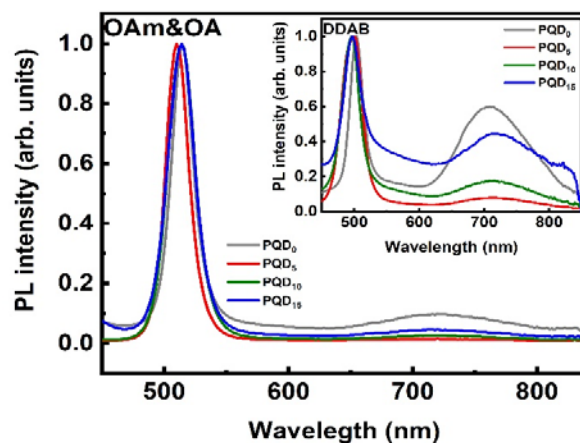


Fig. 4 PL spectra of CsPbBr3 QDs thin films OAm&OA and DDAB ligands under various plasma treatment time

Fig. 5 displays the PL spectra of PQDs/Perovskite bilayers for different plasma treatment times, demonstrating how the second peak in PL spectra suppressed due to the dominant optical behavior of the perovskite layer as the main active layer. The enlarged FWHM observed with increasing plasma treatment time for DDAB ligand suggests its degradation unlike the OAm&OA ligand, which shows greater stability.
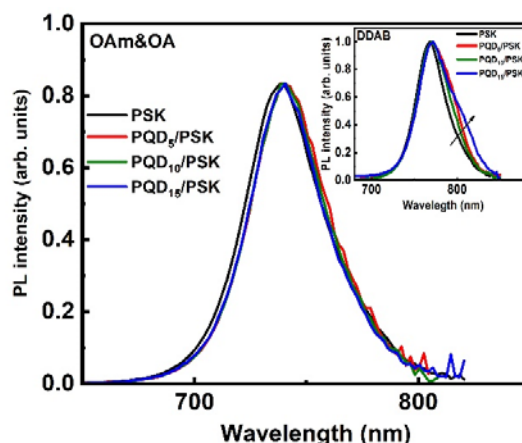


Fig. 5 PL spectra of CsPbBr3 QDs/PSK bilayers with OAm&OA and DDAB ligands for various plasma treatment time

The time-resolved photoluminescence decay curves of PQDs/perovskite bilayers for different durations of plasma treatment are shown in Fig. 6. The unchanged PL lifetime in OAm&OA PQDs/perovskite bilayers is attributed to the stronger quantum confinement and exciton binding energy observed in smaller particles [7]. In particular, smaller QDs lead to shorter exciton diffusion lengths, reducing the probability of recombination and enhancing the overall PL lifetime [6], [8].

World Academy of Science, Engineering and Technology
International Journal of Energy and Power Engineering
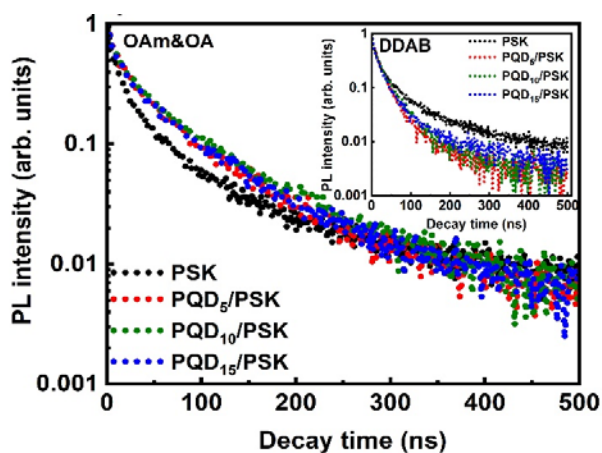Vol:18, No:7, 2024

Fig. 6 Time-resolved photoluminescence decay curves of PQDs/PSK bilayers with OAm&OA and DDAB ligands for different plasma treatment durations

These results highlight the importance of controlling the QD size during synthesis to optimize device performance and stability. In addition, understanding the relationship between QD size and PL lifetime can outline strategies for designing advanced optoelectronic devices utilizing perovskite QDs.

## IV. CONCLUSION

In summary, plasma treatment duration remarkably affects CsPbBr3 quantum dot bilayers depending on the type of surfactant. The post_treatment OAm&OA CsPbBr3 QDs display uniform size distribution, indicating ligand removal and enhanced homogeneity, whereas DDAB CsPbBr3 QDs show intensity fluctuations, suggesting an interplay among ligand removal, QDs aggregation, and surface property changes. The O3 plasma treatment shows greater stability of PQDs with OAm&OA ligand exhibiting no shift of PL peak compared to PQDs with DDAB, specially at shorter exposure times. These results underscore the critical role of ligands in controlling the PQDs stability and morphology during plasma treatment.

## ACKNOWLEDGMENT

## REFERENCES

[1] J. Zou, M. Li, X. Zhang, and W. Zheng, "Perovskite quantum dots: Synthesis, applications, prospects, and challenges," *J. Appl. Phys.*, vol. 132, no. 22, p. 220901, Dec. 2022, doi: 10.1063/5.0126496/2837804.

[2] S. Li *et al.*, "Fostering the Dense Packing of Halide Perovskite Quantum Dots through Binary-Disperse Mixing," *ACS Nano*, vol. 17, no. 20, pp. 20634–20642, Oct. 2023, doi: 10.1021/ACSNANO.3C07688/ASSET/IMAGES/LARGE/NN3C07688_0004.JPEG.

[3] S. Ding, M. Hao, T. Lin, Y. Bai, and L. Wang, "Ligand engineering of perovskite quantum dots for efficient and stable solar cells," *J. Energy Chem.*, vol. 69, pp. 626–648, Jun. 2022, doi: 10.1016/J.JECHEM.2022.02.006.

[4] C. Bi, S. Wang, W. Wen, J. Yuan, G. Cao, and J. Tian, "Room-Temperature Construction of Mixed-Halide Perovskite Quantum Dots with High Photoluminescence Quantum Yield," *J. Phys. Chem. C*, vol. 122, no. 9, pp. 5151–5160, Mar. 2018, doi: 10.1021/ACS.JPCC.7B12607.

[5] J. Wang *et al.*, "Improvement of the Stability and Optical Properties of CsPbBr3 QDs," *Nanomater. 2023, Vol. 13, Page 2372*, vol. 13, no. 16, p. 2372, Aug. 2023, doi: 10.3390/NANO13162372.

[6] S. C. Boehme *et al.*, "Strongly Confined CsPbBr3 Quantum Dots as Quantum Emitters and Building Blocks for Rhombic Superlattices," *ACS Nano*, vol. 17, no. 3, pp. 2089–2100, Feb. 2023, doi: 10.1021/ACSNANO.2C07677/ASSET/IMAGES/LARGE/NN2C07677_0004.JPEG.

[7] L. Zhang *et al.*, "Ultra-long photoluminescence lifetime in an inorganic halide perovskite thin film," *J. Mater. Chem. A*, vol. 7, no. 39, pp. 22229–22234, Oct. 2019, doi: 10.1039/C9TA07412K.

[8] J. Chen, D. Jia, R. Zhuang, Y. Hua, and X. Zhang, "Rejuvenating Aged Perovskite Quantum Dots for Efficient Solar Cells," *Adv. Mater.*, vol. 36, no. 1, p. 2306854, Jan. 2024, doi: 10.1002/ADMA.202306854.